Visible-Light-Driven Rotation of Molecular Motors in a Dual-Function Metal-Organic Framework Enabled by Energy Transfer.

Wojciech Danowski,[a] Fabio Castiglioni,[b] Andy S. Sardjan,[c] Simon Krause,[a] Lukas Pfeifer,[a] Diederik Roke,[a] Angiolina Comotti,[b] Wesley Browne,[a,c,*] Ben L. Feringa[a,*]

a Centre for Systems Chemistry, Stratingh Institute for Chemistry, University of Groningen, Nijenborgh 4, 9747 AG, Groningen, The Netherlands.

b Department of Materials Science, University of Milano Bicocca, Via R. Cozzi 55, Milano, Italy

c Molecular Inorganic Chemistry Group, Stratingh Institute for Chemistry, University of Groningen, Nijenborgh 4, 9747AG Groningen, The Netherlands

The visible-light driven rotation of an overcrowded-alkene based molecular motor strut in a dual-function metal-organic framework (MOF) is reported. Two types of functional linkers, a palladium-porphyrin photosensitizer and a bispyridine derived molecular motor were used to construct the framework capable of harvesting low-energy green light to power the rotary motion. The molecular motor was introduced in the framework using the post synthetic solvent assisted linker exchange (SALE) method and the structure of the material was confirmed by powder (PXRD) and single crystal X-ray (SC-XRD) diffraction. The large decrease in the phosphorescence lifetime and intensity of the porphyrin in the MOFs upon introduction of the molecular motor pillars confirms efficient triplet-to-triplet energy transfer between the porphyrin linkers and molecular motor. Near infrared Raman spectroscopy revealed that the visible light driven rotation of the mo-lecular motor proceeds in the solid state at rates similar to those observed in solution.

Introduction

The development of artificial molecular machines and motors allows for the design and construction of tai-lor-made molecular architectures capable of executing precisely controlled nanoscale structural motion.[1–8] Among these artificial systems, overcrowded-alkene based molecular motors attract considerable attention due to their chirality controlled photochemically-driven repetitive unidirectional rotary motion.[9–11] Alt-hough it has been demonstrated that these molecules can perform various tasks in solution, such as control over the stereochemical outcome of catalytic reac-tions,[12] Brownian motion precludes the cooperative action required to achieve functions beyond molecular dimensions.[5,8,13,14] Achieving ensemble action with artificial molecular machines therefore requires that the randomizing effects of the thermal motion are eliminated by assembly on surfaces[24–26] or integration in the larger systems.[14] Incorporation and immobiliza-tion of these molecules in various supramolecular architectures, including organo[15]- and hydrogels,[16,17]
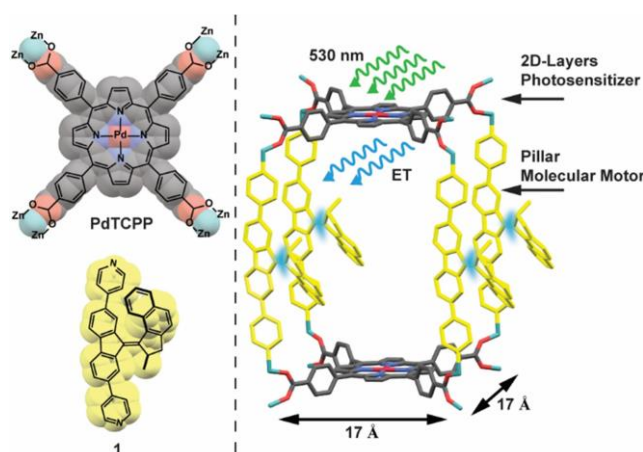

Figure 1 Structures of **PdTCPP** (left, top) and bispyridyl molecular motor **1** (left, bottom) used as linkers for construc-tion of the MOF framework and the schematic representa-tion of the rotation of molecular motor **1** incorporated as struts in the motorized pillared-paddlewheel **PdTCPP** MOF driven by energy transfer from a **PdTCPP** sensitizer (right). Relevant approximate dimensions of the unit cell are given.

polymers,[18,19] liquid crystals[20–23] or self-assembled monolayers[24–26] provided a way to amplify and har- ness their light-induced rotational motion to form responsive materials with tunable properties, includ- ing adaptive polymers,[18,19,27,28] artificial muscles,[16,17] and responsive surfaces.[29] For overcrowded alkene- based materials the use of UV light to drive the mo- lecular motion limits such efforts, due to limited pene- tration depth (due to the scattering), and potential damage by destructive photochemical processes.[11,30,31] Therefore, development of reliable and practical visi- ble-light excitation strategies that are compatible with a chosen material, represents a major challenge cru- cial for further advancement of these dynamic sys- tems.

The most common approaches to red-shifting of the excitation wavelength of the overcrowded alkene- based molecular motors are based on HOMO-LUMO gap engineering featuring extension of the aromatic system,[32] functionalization with donor-acceptor sub- stituents[33,34] or formation of metal complexes.[35] Alt- hough successful, these approaches may reduce the quantum yield of photoisomerization,[32] and are so far limited in the absorption shift (only to the blue part of the visible spectrum; maximum of absorption ca. 450 nm).[34] Furthermore the resulting molecular architec- tures are synthetically more challenging to incorpo- rate in a given material scaffold.[32,35,36] An alternative approach, to achieve visible-light driven rotation of these molecules, is to take advantage of intra- or in- termolecular sensitization through triplet energy trans- fer from a second chromophore.[37] This strategy not only reduces the synthetic efforts but also allows to tune the excitation wavelength over a broad spectral range limited only by the choice of a photosensitizer and triplet-triplet energy transfer requirements.[38] Fur- thermore, it has been successfully applied to operate several types photoswitches by visible light including, azobenzenes,[39,40] stilbenes,[41,42] dithienylethenes.[43,44]

Metal-organic frameworks (MOFs) constitute a class of hybrid materials composed of inorganic nodes and organic linkers connected in a three-dimensional crys- talline, highly porous network.[45–47] Due to the high inherent porosity in these structures, sufficient inter- nal free volume is present to allow for stimuli- responsive structural transformations,[48–57] or rotation- al[58–64] and translational[65] motion of parts of the organ- ic linkers organized in the crystalline solid. In addi- tion, the structural diversity and chemical tunability of these materials makes them ideal platforms to achieve spatial co-organization of functional molecules[66,67] and chromophores.[68] Recent studies on light- harvesting multicomponent MOFs revealed that fac- ile and long-distance energy migration can be

achieved between light-absorbing nodes and/or link- ers in MOFs of various architectures.[69–72] Further- more, the incorporation of photochromic dithi- enylethenes struts in a layered porphyrin MOFs, pro- vided a method for photocontrol over energy transfer between adjacent chromophores and efficiency of singlet oxygen generation.[73,74]

Recently we have demonstrated that a molecular mo- tor incorporated as a strut in a pillared-paddlewheel MOF is capable of performing unhindered, large am- plitude unidirectional rotary motion fueled by UV light and heat.[75] In the present study we show that such rotary motion can be driven by visible light through linker-to-linker energy transfer. The frame- work was constructed from two functional linkers: a porphyrin used as both linker dictating the connectivi- ty of the framework and light-harvesting unit, and a bispyridyl derived molecular motor serving as a pillar and able to undergo rotary motion (Figure 1). In the resulting supramolecular architecture the backbone of the framework is not only a passive 'scaffolding' but plays an active role by absorbing visible light and transferring the collected energy to the molecular motor struts thus driving its rotary motion. This dual- function MOF was obtained using a post-synthetic functionalization method from a parent Zn pillared- paddlewheel MOF bearing palladium porphyrin tetra- carboxylic acid linker (**PdTCPP**) (Figure 1, top left panel) and bispyridyl pillars (Figure 1, bottom left panel). The chosen MOF scaffold provides proximity of both linkers allowing for efficient energy transfer between the chromophores and the large free volume that is essential for unhindered rotation of the light driven molecular motor in the solid state (Figure 1). A key challenge, presented by this approach, is in demonstrating the functioning of the material by spec- troscopic methods due to the overwhelming spectro- scopic properties of the porphyrin chromophore. This unit, which is central to the visible-light driven func- tionality, also precludes standard spectroscopic analy- sis of the motor function, however, near infrared Ra- man spectroscopy (1064 nm) enables full characteri- zation of the motor function.

Results and discussion.

Design, Synthesis and Characterization of a Mo- torized Metal-Organic Framework. For the desired MOF a zinc pillared-paddlewheel scaffold was used, related to the framework we reported recently.[75] In the chosen structure, the nodes of the framework, that is the zinc paddlewheel clusters, are connected by por- phyrin tetracarboxylic acid linkers (**PdTCPP**) form- ing two-dimensional layers, which are pillared by the bispyridine derived linker **1** (Figure 1). We designed the
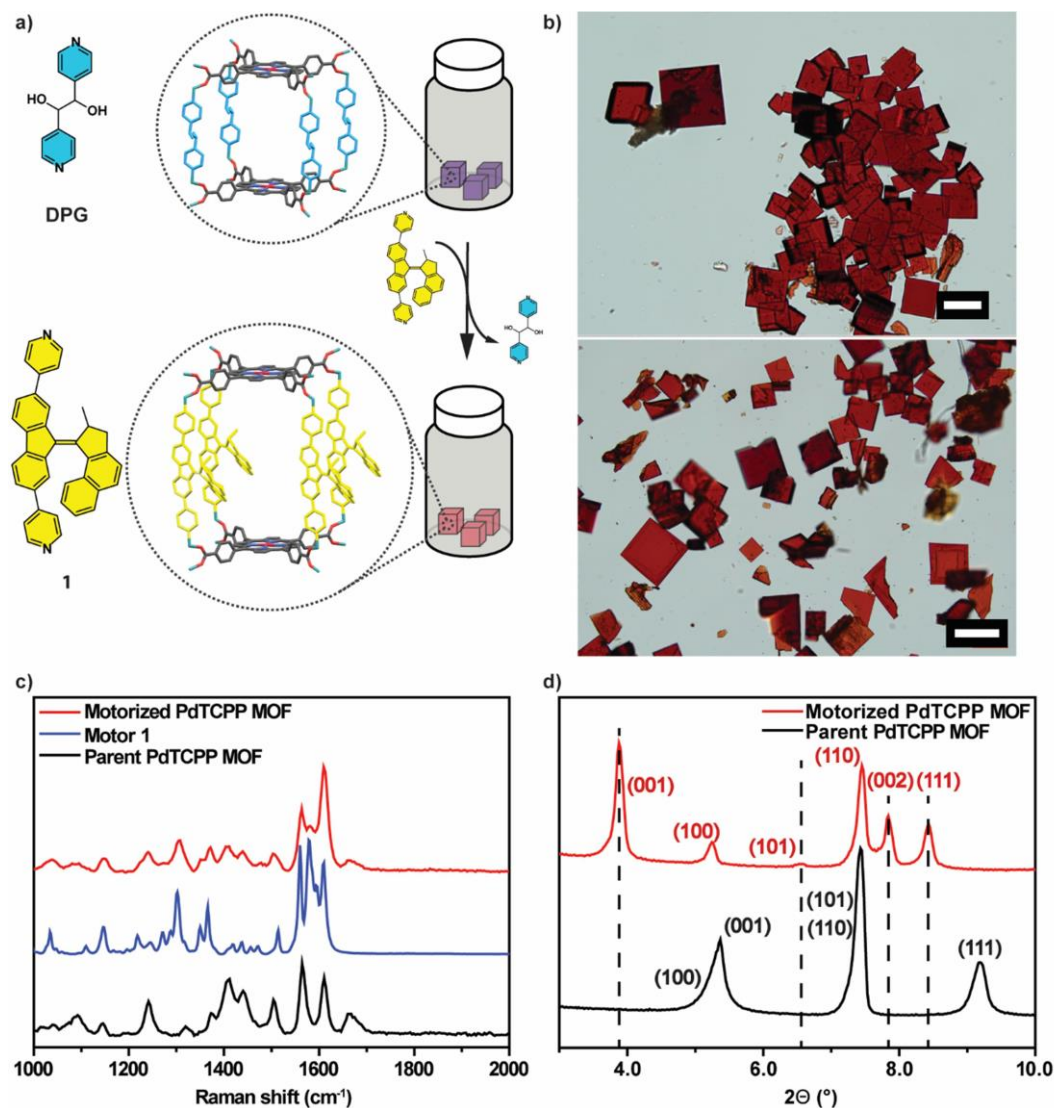
Figure 2 (**a**) Synthesis of the motorized pillared-paddlewheel MOF via SALE from parent MOF bearing **DPG** pillars by exchange with molecular motor **1**. (**b**) Optical micrograph of the parent **PdTCPP DPG**-based MOF (top panel) and motorized **PdTCPP 1**-based MOF (bottom panel) crystals obtained via linker exchange (SALE) (scale bar 100 µm). (**c**) Raman spectra of the parent pillared-paddlewheel MOF (black spectrum, 1064 nm, 250 mW), bispyridyl molecular motor (blue spectrum, 750 nm, 50 mW) and motorized pillared-paddlewheel MOF (red spectrum, 1064 nm, 250 mW). (**d**) Comparison of the experimental PXRD pat- terns of parent MOF (black, bottom pattern) and motorized MOF (red, top pattern). The Miller indices of planes corresponding to the peaks are given in brackets. The vertical dashed lines indicate peaks in PXRD pattern of motorized MOF, corresponding to (*hkl*) (where $l \neq 0$) planes.

system in such a way, that the size of **PdTCPP** linker will ensure sufficient lateral separation of the pillars bearing a molecular motor function, generating free volume critical for uncompromised rotation of the molecular motor (in the designed structure, the distance between the nodes in [100] and [010] planes is approximately 17 Å, Figure 1). Furthermore, the length of bispyridyl derived molecular motor pillar **1** (N-N distance 15.6 Å[75]) should separate the porphyrin layers sufficiently to prevent competing interlayer

porphyrin-porphyrin exciton transport. Finally, the nodes of the framework were based on closed-shell d^{10} configuration Zn^{2+} cations in order to exclude any undesired energy transfer between **PdTCPP** and nodes. Since, MOFs of this topology are typically synthesized under relatively harsh conditions with the presence of strong mineral acids[76], it was decided to prepare the final material using a post-synthetic method i.e. solvent assisted linker exchange (SALE) developed by Farha and Hupp.[77–81] In this process,
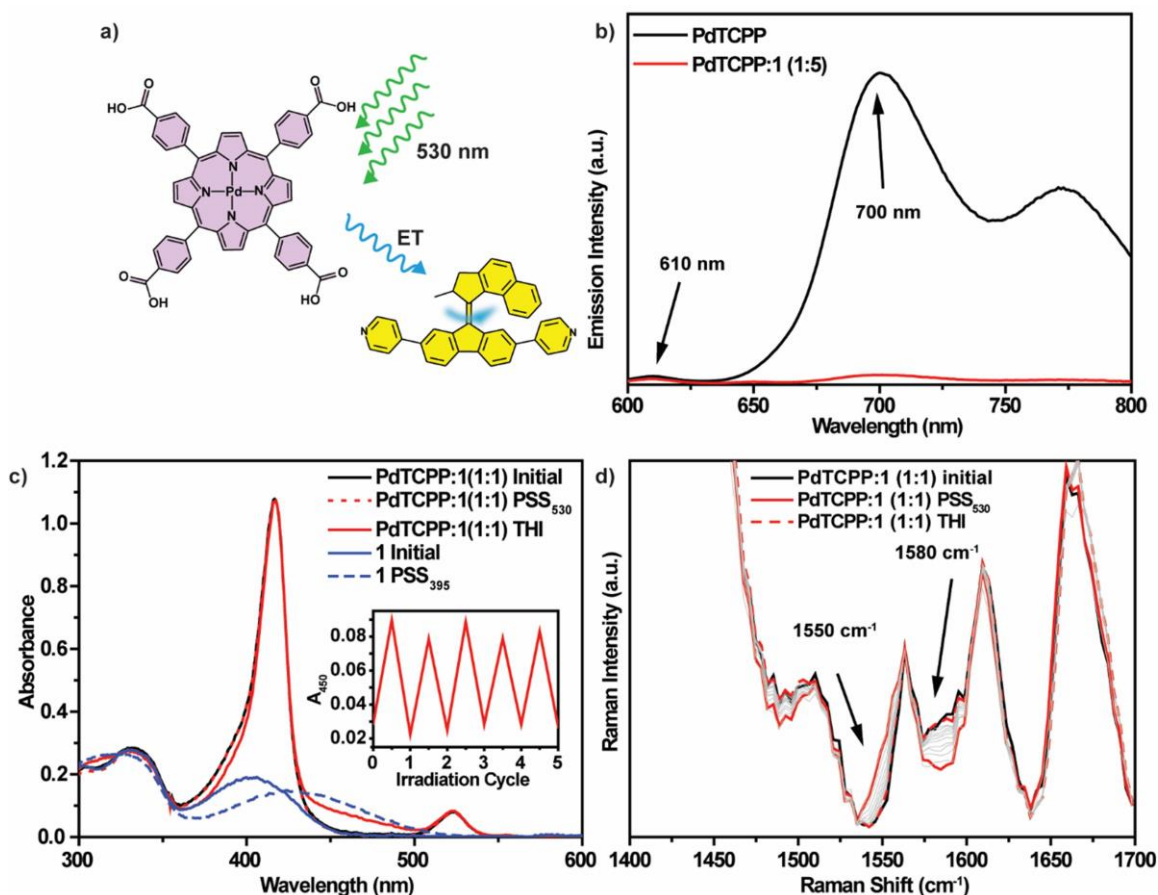
Figure 3 (**a**) Triplet-triplet sensitization of the light driven rotary motion of molecular motor **1** by intermolecular energy transfer from **PdTCPP**. (**b**) Emission spectra ($\lambda_{exc} = 530$ nm) of **PdTCPP** (black spectrum, 44.6 µM, DMF) and a mixture of **PdTCPP** and molecular motor **1** (red spectrum, 1:5 molar ratio of **PdTCPP**:**1**). The emission maxima of fluorescence (610 nm) and phosphorescence (700 nm) are indicated with arrows. (**c**) UV/Vis absorption spectra (-20 °C, 6.1 µM, DMF) of **1** (blue solid line) irradiated at 395 nm to photostationary state (blue dashed line), a mixture of **PdTCPP** and **1** (1:1 molar ratio, black solid line), a mixture of **PdTCPP** and **1** irradiated at 530 nm to the photostationary state (red solid line) and photostationary state mixture after thermal helix inversion (red dashed line). Inset shows changes in absorbance followed at 450 nm upon multiple irradiations and heating cycles. (**d**) Changes in the Raman spectrum (1064 nm, 250 mW) of a mixture of **PdTCPP** and **1** in DMF (black solid line), after irradiation at 530 at -20 °C to a photostationary state (red solid line) and after thermal helix inversion (red dashed line). Arrows indicate bands characteristic of the metastable isomer.

bispyridine derived pillars of the pillared MOFs can be exchanged for different bispyridyl linkers of simi- lar length under neutral conditions, which prevents side reactions and decomposition of the acid-sensitive linkers.[77] Furthermore, it was demonstrated that with this method shorter pillars can also be exchanged for longer pillars thereby making this approach suitable for fabrication of MOFs with larger unit cell parame- ters.[79] Facing the problem of the absence of literature precedents for suitable MOF scaffolds that could serve as a parent MOF for the SALE process in the present design, first a novel MOF bearing *meso*-α,β- di(4-pyridyl) glycol (**DPG**, see Figure 2a for struc- ture) pillar was prepared. The desired pillared- paddlewheel framework was synthesized in a sol- vothermal reaction between **PdTCPP**, **DPG**, $Zn(NO_3)_2 \cdot 6H_2O$ and tetrafluoroboric acid in a binary

solvent mixture (DMF/EtOH) and providing square-shaped crystals (Figure 2b, top panel). It is of note that when the reaction was carried out under less acid- ic conditions predominantly needle-like crystals (Fig- ure S7a) of a three-fold interpenetrated framework with zig-zag structure were obtained (Figure S7b). Characterisation by ^{1}H NMR (d_6-DMSO) spectrosco- py of the digested (using D_2SO_4) square-shape crys- tals of the pillared-paddlewheel MOF showed the expected 1:1 ratio of **DPG** and **PdTCPP** linkers (Fig- ure S1, S2). The initial refinement of the single crystal (SC) X-ray diffraction data collected from the target MOF revealed the expected layered structure com- posed of **PdTCPP** and **Zn** cations, while the **DPG** pillars could not be resolved, presumably due to rota- tional disorder (Figure S5). Nevertheless, the interlay- er distance of 9.2 Å (N-N distance between pyridyl

nitrogens coordinated to paddle-wheel clusters) determined from the structure, corresponded well with the N-N distance (9.4 Å, see SI section 12) in the **DPG** linker, indicating that **DPG** pillars are intercalat- ing the layers of the framework (Figure S5). The powder X-Ray diffraction data (PXRD), acquired under solvent saturated conditions, corroborated bulk crystallinity and phase purity of the sample (Figure 2d, S8). Furthermore, Pawley refinement showed negligible differences between the experimental and simulated diffraction patterns, further indicating the formation of the target pillared structure (Figure S5, S9, Table S2). Elemental analysis corroborated the anticipated elemental composition of the parent MOF (see SI, section 2). Subsequently, the parent **DPG** pillars were exchanged for bispyridyl molecular mo- tor **1**, by means of SALE (Figure 2a), which was car- ried out by soaking the crystals of parent MOF in a DMF solution of bispyridyl molecular motor **1** at 80 °C for 48 h (the solution of **1** was replaced with a fresh solution after 24 h) to achieve full exchange as indicated by ^{1}H NMR spectroscopy of digested crys- tals (Figure 2b bottom panel, S1, S3). Comparison of the Raman spectra of parent and motorized **PdTCPP** MOFs revealed the presence of additional bands char- acteristic of molecular motor **1** in the spectrum of motorized MOF further supporting the successful exchange of the pillars (Figure 2c). As with the parent MOF, the SC X-ray structure of motorized MOF could only be partially resolved. From the refinement of the data the **PdTCPP** units and Zn paddle-wheel clusters forming a layered structure could be con- firmed, while the disorder between the layers preclud- ed the interpretation of electron density of the interca- lating units (Figure S6). Nevertheless, the clear in- crease in the interlayer distance to 15.7 Å (N-N dis- tance between pyridyl nitrogens coordinated to pad- dle-wheel clusters), corroborated the incorporation of longer pillars, consistent with length of the molecular motor **1** (N-N distance in DFT optimized structure B3LYP/6-31G(d,p) 15.4 Å).[75] In addition, the expan- sion of the elementary unit cell in the [001] direction was confirmed by the changes observed in positions of the peaks in the PXRD diffractograms. In compari- son to the PXRD of the parent MOF, significant shifts to a smaller diffraction angle were observed for the peaks ascribed to reflections from planes perpendicu- lar and oblique to the [001] direction, while peaks corresponding to reflections from planes parallel to the [001] direction remained unchanged (Figure 2d, S8). Furthermore, Pawley refinement showed good agreement between the dimensions of the targeted motorized **PdTCPP** MOF unit cell and the experi- mental PXRD pattern (Figure S8, S9, Table S2). Fi- nally, elemental analysis was consistent with the an-

ticipated elemental composition of the parent MOF (see SI, section 2).

Energy transfer, photochemical and thermal isom- erization in solution. Intermolecular energy transfer between the porphyrin (**PdTCPP**) and molecular motor **1** in solution was characterized by emission spectroscopy (Figure 3b). Deoxygenated solutions of **PdTCPP** excited at 530 nm show weak fluorescence at 610 nm and a strong emission band characteristic of phosphorescence at 700 nm (Figure 3b, black line) with a lifetime of ca. 221 µs (Figures S14-16, Table S3).[82] For mixtures of **PdTCPP** and molecular motor **1** (1:5 ratio of **PdTCPP**:**1**) the intensity of the phos- phorescence was substantially reduced with a de- crease in phosphorescence lifetime to ca. 5 µs (Figure S14-16, Table S3), in line with energy transfer be- tween triplet states of the porphyrin and motor **1** (Fig- ure 3b, red line). Stern-Volmer plots (emission inten- sity and lifetime, Figures S14 and S16, respectively) with concentrations of **1** between 0.0 and 223.0 µM were linear confirming dynamic quenching of the phosphorescence of **PdTCPP** thus excluding for- mation of aggregates in the concentration range stud- ied. Linear fitting of the data gave an intermolecular quenching rate constant $k_q = 0.9 \cdot 10^9$ M^{-1} s^{-1} closely matching the diffusion-limited rate constant in DMF ($7.6 \cdot 10^9$ M^{-1} s^{-1} at 20 °C),[83] suggesting that the energy transfer between **PdTCPP** and **1** is under diffusion control (Figure S14, S16).

Intermolecular sensitization of the rotary motion of motor **1** in solution was studied with UV/Vis absorp- tion, ^{1}H NMR and Raman spectroscopies (Figure 3c,d Figure S4). In the UV/Vis absorption spectra the re- gion characteristic of the main absorption band of the molecular motor **1** (maximum ~ 400 nm, Figure 3c, blue solid line) is dominated by the strong Soret band of **PdTCPP** (Figure 3c, black solid line). Neverthe- less, irradiation of the argon purged solution of **1** and **PdTCPP** (1:1 ratio of **1**:**PdTCPP**) at 530 nm (Q band of the porphyrin) led to a bathochromic shift of the absorption in the region of the Soret band (Figure 3c, red solid line), consistent with the formation of the metastable isomer of molecular motor (Figure 3c, blue dashed lines). Subsequent warming of the sample led to the recovery of the original spectrum, con- sistent with the recovery of the stable isomer by ther- mal helix inversion (Figure 3b, red dashed line). An isosbestic point was maintained at 323 nm throughout both photochemical and thermal processes, as ex- pected for unimolecular reactions (Figure S12). Fur- thermore, the irradiation/thermal isomerization cycles could be performed for at least five consecutive cy- cles without noticeable fatigue or degradation (Figure 3c, inset). The rate of the thermal helix inversion of

bispyridyl motor **1** in the presence of **PdTCPP** in DMF was determined following the exponential decrease of the absorbance at 440 nm over a range of temperatures (6-14 °C, Figure S13). Eyring plot anal- ysis showed that the Gibbs free energy of activation of the thermal helix inversion of the metastable iso- mer of **1** in this mixture ($\Delta^{\ddagger}G$(20 °C) = 88.0±0.4 kJ mol^{-1}, $t_{1/2}$ = 9.1 min, Figure S13) is essen- tially the same as the previously determined value in DMF[75] ($\Delta^{\ddagger}G$(20 °C) = 87.7±0.6 kJ mol^{-1}, $t_{1/2}$ = 8.0 min), thereby demonstrating that bispyridyl motor **1** can operate similarly via direct excitation and triplet sensitization. In the Raman spectra of the equimolar mixture of **PdTCPP** and **1** in DMF, bands characteris- tic of **PdTCPP** partially overlap and obscure bands characteristic of **1** (Figure 3d, black spectrum). None- theless, the features consistent with sequential photo- chemical and thermal isomerization of **1** could be readily observed with Raman spectroscopy. Irradia- tion of this mixture at 530 nm at low temperature (- 20 °C, sufficient to prevent thermal helix inversion over the time scale of the experiment) led to a de- crease in the Raman scattering at 1580 cm^{-1} with con- comitant increase at 1550 cm^{-1}. Warming to room temperature led to gradual recovery of the initial spec- trum (Figure 3d). The intermolecular energy transfer induced photoisomerization of motor **1** was monitored with low temperature ^{1}H NMR spectroscopy (Figure S4). After irradiation of an equimolar mixture of **1** and **PdTCPP** at 530 nm at -30 °C, a new set of up- field shifted ^{1}H NMR resonances was observed in the aliphatic part of the spectrum, characteristic of the metastable isomer. Warming the sample resulted in full recovery of the original spectrum and hence of the stable isomer. The photostationary state ratio of metastable and stable isomers of **1**, established upon irradiation at 530 nm, was approximately 1:1 (Figure S4), consistent with changes observed by Raman spectroscopy (Figure 3d), which showed ~ 50 % de- crease in the intensity of the bands characteristic of the stable isomer (1580 cm^{-1}).

Energy transfer, photochemical and thermal isom- erization in the solid state. The extent of the energy transfer between the **1** and **PdTCPP** linkers in motor- ized MOF was determined with steady-state and time- resolved emission spectroscopy. Upon excitation at 530 nm the parent **PdTCPP** MOF showed a similar emission spectrum to that of **PdTCPP** in DMF with a small hypsochromic shift of both fluorescence and phosphorescence (Figure 4a). Conversely, in the emission spectrum of the motorized **PdTCPP** MOF a strong decrease in the phosphorescence intensity was observed, consistent with the energy transfer between the linkers (Figure 4a). Furthermore a significant drop

in the porphyrin phosphorescence lifetime was ob- served from ca. 100 μs for the parent MOF to ca. 10 μs for the motorized MOF, demonstrating efficient
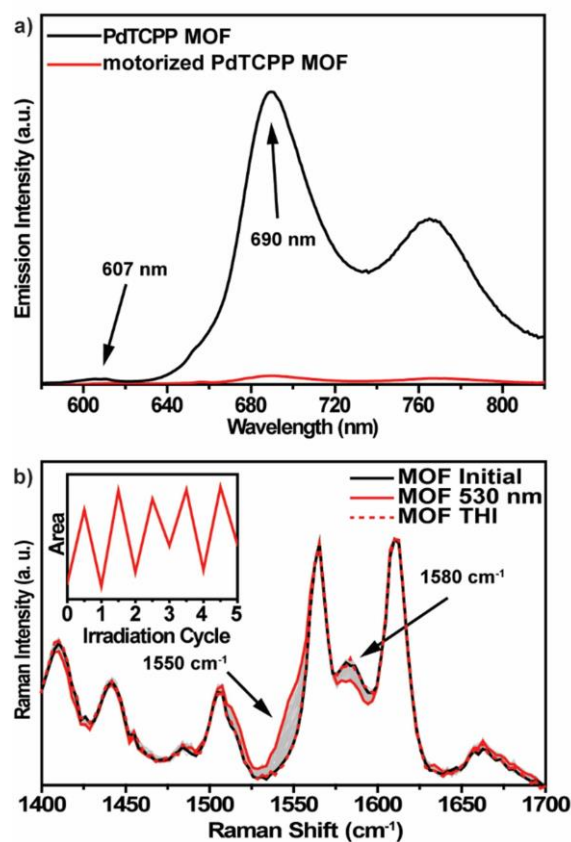

Figure 4 (**a**) Comparison of emission spectra (λ_{exc} = 530 nm) of DMF suspensions of parent **PdTCPP** MOF (black line) and motorized **PdTCPP** MOF (red line). (**b**) Changes in the Ra- man spectrum (1064 nm, 250 mW, 40 s integration time) of the motorized **PdTCPP** MOF sample (black solid line) upon irradiation at 530 nm (red solid line) and subsequent thermal isomerization (red dashed line). Inset shows changes in the area around 1550 cm^{-1} followed upon multiple photochemi- cal/thermal isomerization cycles.

energy transfer between the **1** and **PdTCPP** linkers in MOF (Figure S17, S18). The rotary motion of motor **1** inserted in the MOF scaffold was followed with NIR- Raman spectroscopy (see SI section 12 for other spec- tra). Previously, we demonstrated that this technique is particularly convenient to study the photochemical and thermal isomerization of rotary molecular motors in condensed phase as it allows for unambiguous cor- relation of spectral data with the structural changes that these molecules exhibit in response to light and heat stimuli.[75] Upon exposure of the polycrystalline motorized **PdTCPP** MOF sample to green light (530 nm) a gradual decrease in the Raman intensity at 1580 cm^{-1} with concomitant increase in scattering intensity at 1550 cm^{-1} was observed (Figure 4b). Similar spectral features were detected upon photo-

chemical isomerization of molecular motor **1** in solution and therefore could be ascribed to the same photochemical process. Furthermore, Raman spectrosco- py showed that, for thin samples (much less than 100 µm), the photostationary state of **1** reached via triplet sensitization in motorized **PdTCPP** MOF was similar to that in solution (Figure S22). When the irradiation was discontinued, the initial Raman spec- trum was recovered gradually indicating thermal re- laxation of the metastable to stable isomer. The barrier of the thermal relaxation at room temperature was determined by monitoring the changes in the bands area characteristic of the metastable isomer (Figures S23-25 and Table S3). The Gibbs free energy of acti- vation for this process ($\Delta^{\ddagger}G(20\ °C)$) was $88.7\pm0.8\ \mathrm{kJ\ mol^{-1}}$, $t_{1/2}$ ~ 13 min) and corresponded well to the barrier determined in DMF solution ($88.0\pm0.4\ \mathrm{kJ\ mol^{-1}}$, $t_{1/2}$ ~ 9 min). The good agreement between the barriers in the solution and the solid ma- terial shows that molecular motor **1** can perform its large amplitude rotary motion uncompromised while incorporated in **PdTCPP** MOF. Furthermore, irradia- tion/thermal relaxation steps could be repeated over five cycles (Figure 4b, inset) without any noticeable sign of fatigue or photo-degradation indicating high stability of the framework.

Conclusions

In conclusion we have established that the photoisomerization of the molecular motor pillars in a porphyrin Zn-paddlewheel MOF can be driven with visible light by triplet sensitization. The desired motorized MOF was constructed by post synthetic linker exchange (SALE) from the newly developed parent **PdTCPP** MOF bearing **DPG** pillars. Exchange of these pillars with the longer bispyridyl motor **1** result- ed in the expected expansion of the elementary cell in the *c* direction as shown by the SC X-ray and PXRD data. Due to the spatial co-arrangement of the chro- mophores in the motorized MOF, the energy transfer between photosensitizer (2D layers) and molecular motor (pillars) was found to be efficient, and the pho- tochemical isomerization of the molecular motor could be achieved with green 530 nm light. Addition- ally, it was shown that the rate of the thermal helix inversion step of the molecular motors incorporated in the material scaffold is essentially the same as that observed in solution, owing to the large free volume present in the framework. The demonstration of visi- ble light driven rotary motion of a molecular motor in a metal-organic framework, opens many perspectives for future applications such as membranes and pumps able to accelerate flow of gases or in combination with catalytic function, miniaturized chemical reac-

tors able to accelerate inflow of reactants and outflow of products, powered by non-invasive visible light.[84] Furthermore, we envision that this strategy may be used to expand the scope of photosensitizers and mo- lecular motors to achieve even further shift of the excitation wavelength towards red light.

ASSOCIATED CONTENT

Synthetic procedures and characterization, additional UV/vis and Raman spectra, Eyring plot, details on quantum yield and life time determination

AUTHOR INFORMATION

Corresponding Author

* B.L.Feringa@rug.nl

* W.R.Browne@rug.nl

Author Contributions

W.D., F.C. synthesized MOFs; W.D. performed PXRD; W.D. analyzed rotary motion of motor in solution; W.D., A.S.S. performed emission studies in solution and solid state; S.K. performed Pawley refinement; L.P. performed SC X-Ray studies; W.D., W.R.B. studied the rotary motion in solid. W.D., W.R.B, B.L.F. conceived the project; W.R.B., B.L.F., A. C., guided the project; W.D., W.R.B., B.L.F. wrote the manu- script; all authors discussed the results and commented on the manuscript.

Notes
The authors declare no competing financial interest.

ACKNOWLEDGMENT

REFERENCES

(1) Dietrich-Buchecker, C.; Jimenez-Molero, M. C.; Sartor, V.; Sauvage, J.-P. Rotaxanes and Catenanes as Prototypes of Molecular Machines and Motors. *Pure Appl. Chem.* **2003**, *75* (10), 1383–1393.

(2) Bruns, C. J.; Stoddart, J. F. *The Nature of the Mechanical Bond: From Molecules to Machines*; Wiley: Hoboken, NJ, USA, 2016.

(3) Balzani, V.; Venturi, M.; Credi, A. *Molecular Devices and Machines : A Journey into the Nano World*; Wiley-VCH: Weinheim, 2003.

(4) Schliwa, M. *Molecular Motors*; Wiley-VCH: Weinheim, 2003.

(5) Kinbara, K.; Aida, T. Toward Intelligent Molecular Machines: Directed Motions of Biological and Artificial

Molecules and Assemblies. *Chem. Rev.* **2005**, *105*, 1377–1400.

(6) Erbas-Cakmak, S.; Leigh, D. A.; McTernan, C. T.; Nussbaumer, A. L. Artificial Molecular Machines. *Chem. Rev.* **2015**, *115* (18), 10081–10206.

(7) García-López, V.; Liu, D.; Tour, J. M. Light-Activated Organic Molecular Motors and Their Applications. *Chem. Rev.* **2020**, *120* (1), 79–124.

(8) Browne, W. R.; Feringa, B. L. Making Molecular Machines Work. *Nat. Nanotechnol.* **2006**, *1* (1), 25–35.

(9) Koumura, N.; Zijistra, R. W. J.; van Delden, R. A.; Harada, N.; Feringa, B. L. Light-Driven Monodirectional Molecular Rotor. *Nature* **1999**, *401* (6749), 152–155.

(10) Koumura, N.; Geertsema, E. M.; Meetsma, A.; Feringa, B. L. Light-Driven Molecular Rotor: Unidirectional Rotation Controlled by a Single Stereogenic Center. *J. Am. Chem. Soc.* **2000**, *122* (48), 12005–12006.

(11) van Leeuwen, T.; Lubbe, A. S.; Štacko, P.; Wezenberg, S. J.; Feringa, B. L. Dynamic Control of Function by Light-Driven Molecular Motors. *Nat. Rev. Chem.* **2017**, *1*, 96.

(12) Wang, J.; Feringa, B. L. Dynamic Control of Chiral Space in a Catalytic Asymmetric Reaction Using a Molecular Motor. *Sci.* **2011**, *331* (6023), 1429–1432.

(13) Astumian, R. D. Design Principles for Brownian Molecular Machines: How to Swim in Molasses and Walk in a Hurricane. *Proc. Natl. Acad. Sci., U. S. A* **2006**, *46* (37), 10771–10776.

(14) Coskun, A.; Banaszak, M.; Astumian, R. D.; Stoddart, J. F.; Grzybowski, B. A. Great Expectations: Can Artificial Molecular Machines Deliver on Their Promise? *Chem. Soc. Rev.* **2012**, *41* (1), 19–30.

(15) Wezenberg, S. J.; Croisetu, C. M.; Stuart, M. C. A.; Feringa, B. L. Reversible Gel–sol Photoswitching with an Overcrowded Alkene-Based Bis-Urea Supergelator. *Chem. Sci.* **2016**, *7* (7), 4341–4346.

(16) Chen, J.; Leung, F. K. C.; Stuart, M. C. A.; Kajitani, T.; Fukushima, T.; van der Giessen, E.; Feringa, B. L. Artificial Muscle-like Function from Hierarchical Supramolecular Assembly of Photoresponsive Molecular Motors. *Nat. Chem.* **2018**, *10* (2), 132–138.

(17) Leung, F. K.-C.; van den Enk, T.; Kajitani, T.; Chen, J.; Stuart, M. C. A.; Kuipers, J.; Fukushima, T.; Feringa, B. L. Supramolecular Packing and Macroscopic Alignment Controls Actuation Speed in Macroscopic Strings of Molecular Motor Amphiphiles. *J. Am. Chem. Soc.* **2018**, *140* (50), 17724–17733.

(18) Li, Q.; Fuks, G.; Moulin, E.; Maaloum, M.; Rawiso, M.; Kulic, I.; Foy, J. T.; Giuseppone, N. Macroscopic Contraction of a Gel Induced by the Integrated Motion of Light-Driven Molecular Motors. *Nat. Nanotechnol.* **2015**, *10* (2), 161–165.

(19) Foy, J. T.; Li, Q.; Goujon, A.; Colard-Itté, J. R.; Fuks, G.; Moulin, E.; Schiffmann, O.; Dattler, D.; Funeriu, D. P.; Giuseppone, N. Dual-Light Control of Nanomachines That Integrate Motor and Modulator Subunits. *Nat. Nanotechnol.* **2017**, *12* (6), 540–545.

(20) Eelkema, R.; Pollard, M. M.; Vicario, J.; Katsonis, N.; Ramon, B. S.; Bastiaansen, C. W. M.; Broer, D. J.; Feringa, B. L. Nanomotor Rotates Microscale Objects. *Nature* **2006**, *440* (7081), 163.

(21) Pijper, D.; Jongejan, M. G. M.; Meetsma, A.; Feringa, B. L. Light-Controlled Supramolecular Helicity of a Liquid Crystalline Phase Using a Helical Polymer Functionalized with a Single Chiroptical Molecular Switch. *J. Am. Chem. Soc.* **2008**, *130* (13), 4541–4552.

(22) Orlova, T.; Lancia, F.; Loussert, C.; Iamsaard, S.; Katsonis, N.; Brasselet, E. Revolving Supramolecular Chiral Structures Powered by Light in Nanomotor-Doped Liquid Crystals. *Nat. Nanotechnol.* **2018**, *13* (4), 304–308.

(23) Zou, C.; Sun, J.; Wang, M.; Wang, J.; Wu, Y.; Zhang, L.; Zhu, Z.; Xiong, G.; Jiang, L.; Ikeda, T.; et al. A UV-Responsive Multifunctional Photoelectric Device Based on Discotic

Columnar Nanostructures and Molecular Motors. *Adv. Mater.* **2019**, *31* (8), 1806016.

(24) Carroll, G. T.; London, G.; Landaluce, T. F.; Rudolf, P.; Feringa, B. L. Adhesion of Photon-Driven Molecular Motors to Surfaces *via* 1,3-Dipolar Cycloadditions: Effect of Interfacial Interactions on Molecular Motion. *ACS Nano* **2011**, *5* (1), 622–630.

(25) van Delden, R. A.; ter Wiel, M. K. J.; Pollard, M. M.; Vicario, J.; Koumura, N.; Feringa, B. L. Unidirectional Molecular Motor on a Gold Surface. *Nature* **2005**, *437* (7063), 1337–1340.

(26) Kaleta, J.; Chen, J.; Bastien, G.; Dračínský, M.; Mašát, M.; Rogers, C. T.; Feringa, B. L.; Michl, J. Surface Inclusion of Unidirectional Molecular Motors in Hexagonal Tris(o-Phenylene)cyclotriphosphazene. *J. Am. Chem. Soc.* **2017**, *139* (30), 10486–10498.

(27) van Leeuwen, T.; Heideman, G. H.; Zhao, D.; Wezenberg, S. J.; Feringa, B. L. In Situ Control of Polymer Helicity with a Non-Covalently Bound Photoresponsive Molecular Motor Dopant. *Chem. Commun.* **2017**, *53* (48), 6393–6396.

(28) Pijper, D.; Feringa, B. L. Molecular Transmission: Controlling the Twist Sense of a Helical Polymer with a Single Light-Driven Molecular Motor. *Angew. Chem. Int. Ed.* **2007**, *46* (20), 3693–3696.

(29) Chen, K. Y.; Ivashenko, O.; Carroll, G. T.; Robertus, J.; Kistemaker, J. C. M.; London, G.; Browne, W. R.; Rudolf, P.; Feringa, B. L. Control of Surface Wettability Using Tripodal Light-Activated Molecular Motors. *J. Am. Chem. Soc.* **2014**, *136* (8), 3219–3224.

(30) Russew, M.-M.; Hecht, S. Photoswitches: From Molecules to Materials. *Adv. Mater.* **2010**, *22* (31), 3348–3360.

(31) Lubbe, A. S.; van Leeuwen, T.; Wezenberg, S. J.; Feringa, B. L. Designing Dynamic Functional Molecular Systems. *Tetrahedron* **2017**, *73* (33), 4837–4848.

(32) van Leeuwen, T.; Pol, J.; Roke, D.; Wezenberg, S. J.; Feringa, B. L. Visible-Light Excitation of a Molecular Motor with an Extended Aromatic Core. *Org. Lett.* **2017**, *19* (6), 1402–1405.

(33) van Delden, R. A.; Koumura, N.; Schoevaars, A.; Meetsma, A.; Feringa, B. L. A Donor–acceptor Substituted Molecular Motor: Unidirectional Rotation Driven by Visible Light. *Org. Biomol. Chem.* **2003**, *1* (1), 33–35.

(34) Pfeifer, L.; Scherübl, M.; Fellert, M.; Danowski, W.; Cheng, J.; Pol, J.; Feringa, B. L. Photoefficient 2nd Generation Molecular Motors Responsive to Visible Light. *Chem. Sci.* **2019**, *10* (38), 8768–8773.

(35) Wezenberg, S. J.; Chen, K.-Y.; Feringa, B. L. Visible-Light-Driven Photoisomerization and Increased Rotation Speed of a Molecular Motor Acting as a Ligand in a Ruthenium(II) Complex. *Angew. Chemie Int. Ed.* **2015**, *54* (39), 11457–11461.

(36) Roke, D.; Wezenberg, S. J.; Feringa, B. L. Molecular Rotary Motors: Unidirectional Motion around Double Bonds. *Proc. Natl. Acad. Sci.* **2018**, *115* (38), 9423–9431.

(37) Cnossen, A.; Hou, L.; Pollard, M. M.; Wesenhagen, P. V.; Browne, W. R.; Feringa, B. L. Driving Unidirectional Molecular Rotary Motors with Visible Light by Intra- And Intermolecular Energy Transfer from Palladium Porphyrin. *J. Am. Chem. Soc.* **2012**, *134* (42), 17613–17619.

(38) Perego, J.; Pedrini, J.; Bezuidenhout, C. X.; Sozzani, P. E.; Meinardi, F.; Bracco, S.; Comotti, A.; Monguzzi, A. Engineering Porous Emitting Framework Nanoparticles with Integrated Sensitizers for Low-Power Photon Upconversion by Triplet Fusion. *Adv. Mater.* **2019**, *31* (40), 1903309.

(39) Sakamoto, R.; Kume, S.; Sugimoto, M.; Nishihara, H. *Trans - Cis* Photoisomerization of Azobenzene-Conjugated Dithiolato-Bipyridine Platinum(II) Complexes: Extension of Photoresponse to Longer Wavelengths and Photocontrollable Tristability. *Chem.: Eur. J.* **2009**, *15* (6), 1429–1439.

(40) Bischel, . W K; Perry, B. E.; Crosley ; M. Aldén, D. R.; Edner, H.; Grafström, P.; Svanberg, S.; Buijsse, ; B. Magnetic

Bistability of Molecules in Homogeneous Solution at Room Temperature. *Science* **2011**, *331*, 445–448.

(41) Mercer-Smith, J. A.; Whitten, D. G. Photosensitization of Stilbene Isomerization by Palladium and Platinum Porphyrins, an Intermolecular Quantum Chain Process. *J. Am. Chem. Soc.* **1978**, *100* (9), 2620–2625.

(42) Serreli, V.; Lee, C. F.; Kay, E. R.; Leigh, D. A. A Molecular Information Ratchet. *Nature* **2007**, *445* (7127), 523–527.

(43) Jukes, R. T. F.; Adamo, V.; Hartl, F.; Belser, P.; De Cola, L. Photochromic Dithienylethene Derivatives Containing Ru(II) or Os(II) Metal Units. Sensitized Photocyclization from a Triplet State. *Inorg. Chem.* **2004**, *43* (9), 2779–2792.

(44) Yam, V. W.-W.; Ko, C.-C.; Zhu, N. Photochromic and Luminescence Switching Properties of a Versatile Diarylethene-Containing 1,10-Phenanthroline Ligand and Its Rhenium(I) Complex. *J. Am. Chem. Soc.* **2004**, *126* (40), 12734–12735.

(45) Howarth, A. J.; Liu, Y.; Li, P.; Li, Z.; Wang, T. C.; Hupp, J. T.; Farha, O. K. Chemical, Thermal and Mechanical Stabilities of Metal-Organic Frameworks. *Nat. Rev. Mater.* **2016**, *1* (15018), 1–15.

(46) Li, H.; Eddaoudi, M.; O'Keeffe, M.; Yaghi, O. M. Design and Synthesis of an Exceptionally Stable and Highly Porous Metal-Organic Framework. *Nature* **1999**, *402*, 276–279.

(47) Furukawa, H.; Cordova, K. E.; O'Keeffe, M.; Yaghi, O. M. The Chemistry and Applications of Metal-Organic Frameworks. *Science* **2013**, *341* (6149), 1230444.

(48) Jones, C. L.; Tansell, A. J.; Easun, T. L. The Lighter Side of MOFs: Structurally Photoresponsive Metal–organic Frameworks. *J. Mater. Chem. A* **2016**, *4* (18), 6714–6723.

(49) Castellanos, S.; Kapteijn, F.; Gascon, J. Photoswitchable Metal Organic Frameworks: Turn on the Lights and Close the Windows. *CrystEngComm* **2016**, *18* (22), 4006–4012.

(50) McGonigal, P. R.; Deria, P.; Hod, I.; Moghadam, P. Z.; Avestro, A.-J.; Horwitz, N. E.; Gibbs-Hall, I. C.; Blackburn, A. K.; Chen, D.; Botros, Y. Y.; et al. Electrochemically Addressable Trisradical Rotaxanes Organized within a Metal–organic Framework. *Proc. Natl. Acad. Sci.* **2015**, *112* (36), 11161–11168.

(51) Chen, Q.; Sun, J.; Li, P.; Hod, I.; Moghadam, P. Z.; Kean, Z. S.; Snurr, R. Q.; Hupp, J. T.; Farha, O. K.; Stoddart, J. F. A Redox-Active Bistable Molecular Switch Mounted inside a Metal-Organic Framework. *J. Am. Chem. Soc.* **2016**, *138* (43), 14242–14245.

(52) Kolokolov, D. I.; Stepanov, A. G.; Guillerm, V.; Serre, C.; Frick, B.; Jobic, H.; Williams, D. E.; Martin, C. R.; Dolgopolova, E. A.; Swifton, A.; et al. Flipping the Switch: Fast Photoisomerization in a Confined Environment. *J. Am. Chem. Soc.* **2018**, *140* (24), 7611–7622.

(53) Dolgopolova, E. A.; Galitskiy, V. A.; Martin, C. R.; Gregory, H. N.; Yarbrough, B. J.; Rice, A. M.; Berseneva, A. A.; Ejegbavwo, O. A.; Stephenson, K. S.; Kittikhunnatham, P.; et al. Connecting Wires: Photoinduced Electronic Structure Modulation in Metal-Organic Frameworks. *J. Am. Chem. Soc.* **2019**, *141* (13), 5350–5358.

(54) Brown, J. W.; Henderson, B. L.; Kiesz, M. D.; Whalley, A. C.; Morris, W.; Grunder, S.; Deng, H.; Furukawa, H.; Zink, J. I.; Stoddart, J. F.; et al. Photophysical Pore Control in an Azobenzene-Containing Metal–organic Framework. *Chem. Sci.* **2013**, *4* (7), 2858.

(55) Furlong, B. J.; Katz, M. J. Bistable Dithienylethene-Based Metal-Organic Framework Illustrating Optically Induced Changes in Chemical Separations. *J. Am. Chem. Soc.* **2017**, *139* (38), 13280–13283.

(56) Zheng, Y.; Sato, H.; Wu, P.; Jeon, H. J.; Matsuda, R.; Kitagawa, S. Flexible Interlocked Porous Frameworks Allow Quantitative Photoisomerization in a Crystalline Solid. *Nat. Commun.* **2017**, *8* (1), 1–6.

(57) Nikolayenko, V. I.; Herbert, S. A.; Barbour, L. J. Reversible Structural Switching of a Metal-Organic Framework by Photoirradiation. *Chem. Commun.* **2017**, *53* (81), 11142–11145.

(58) Gould, S. L.; Tranchemontagne, D.; Yaghi, O. M.; Garcia-Garibay, M. A. The Amphidynamic Character of Crystalline MOF-5: Rotational Dynamics in a Free-Volume Environment. *J. Am. Chem. Soc.* **2008**, *130* (Figure 3), 3246–3247.

(59) Bracco, S.; Castiglioni, F.; Comotti, A.; Galli, S.; Negroni, M.; Maspero, A.; Sozzani, P. Ultrafast Molecular Rotors and Their CO_2 Tuning in MOFs with Rod-Like Ligands. *Chem.: Eur. J.* **2017**, *23* (47), 11210–11215.

(60) Vogelsberg, C. S.; Uribe-Romo, F. J.; Lipton, A. S.; Yang, S.; Houk, K. N.; Brown, S.; Garcia-Garibay, M. A. Ultrafast Rotation in an Amphidynamic Crystalline Metal Organic Framework. *Proc. Natl. Acad. Sci.* **2017**, *114* (52), 13613–13618.

(61) Jiang, X.; Duan, H.-B.; Khan, S. I.; Garcia-Garibay, M. A. Diffusion-Controlled Rotation of Triptycene in a Metal-Organic Framework (MOF) Sheds Light on the Viscosity of MOF-Confined Solvent. *ACS Cent. Sci.* **2016**, *2* (9), 608–613.

(62) Vukotic, V. N.; Harris, K. J.; Zhu, K.; Schurko, R. W.; Loeb, S. J. Metal-Organic Frameworks with Dynamic Interlocked Components. *Nat. Chem.* **2012**, *4* (6), 456–460.

(63) Zhu, K.; Vukotic, V. N.; Okeefe, C. A.; Schurko, R. W.; Loeb, S. J. Metal-Organic Frameworks with Mechanically Interlocked Pillars: Controlling Ring Dynamics in the Solid-State via a Reversible Phase Change. *J. Am. Chem. Soc.* **2014**, *136* (20), 7403–7409.

(64) Vukotic, V. N.; Keefe, C. A. O.; Zhu, K.; Harris, K. J.; To, C.; Schurko, R. W.; Loeb, S. J. Mechanically Interlocked Linkers inside Metal − Organic Frameworks: Effect of Ring Size on Rotational Dynamics. *J. Am. Chem. Soc.* **2015**, *137*, 9643–9651.

(65) Zhu, K.; O'Keefe, C. A.; Vukotic, V. N.; Schurko, R. W.; Loeb, S. J. A Molecular Shuttle That Operates inside a Metal-Organic Framework. *Nat. Chem.* **2015**, *7* (6), 514–519.

(66) Deng, H.; Doonan, C. J.; Furukawa, H.; Ferreira, R. B.; Towne, J.; Knobler, C. B.; Wang, B.; Yaghi, O. M. Multiple Functional Groups of Varying Ratios in Metal-Organic Frameworks. *Science* **2010**, *327* (5967), 846–850.

(67) Kong, X.; Deng, H.; Yan, F.; Kim, J.; Swisher, J. A.; Smit, B.; Yaghi, O. M.; Reimer, J. A. Mapping of Functional Groups in Metal-Organic Frameworks. *Sci.* **2013**, *341* (6148), 882– 885.

(68) Lee, C. Y.; Farha, O. K.; Hong, B. J.; Sarjeant, A.; Nguyen, S. T.; Hupp, J. T. Light-Harvesting Metal–Organic Frameworks (MOFs): Efficient Strut-to-Strut Energy Transfer in Bodipy and Porphyrin-Based MOFs. *J. Am. Chem. Soc.* **2011**, *133* (40), 15858–15861.

(69) Kent, C. A.; Mehl, B. P.; Ma, L.; Papanikolas, J. M.; Meyer, T. J.; Lin, W. Energy Transfer Dynamics in Metal−Organic Frameworks. *J. Am. Chem. Soc.* **2010**, *132* (37), 12767–12769.

(70) Zhang, X.; Ballem, M. A.; Hu, Z.-J.; Bergman, P.; Uvdal, K. Nanoscale Light-Harvesting Metal-Organic Frameworks. *Angew. Chemie Int. Ed.* **2011**, *50* (25), 5729–5733.

(71) Son, H.-J.; Jin, S.; Patwardhan, S.; Wezenberg, S. J.; Jeong, N. C.; So, M.; Wilmer, C. E.; Sarjeant, A. A.; Schatz, G. C.; Snurr, R. Q.; et al. Light-Harvesting and Ultrafast Energy Migration in Porphyrin-Based Metal–Organic Frameworks. *J. Am. Chem. Soc.* **2013**, *135* (2), 862–869.

(72) So, M. C.; Wiederrecht, G. P.; Mondloch, J. E.; Hupp, J. T.; Farha, O. K. Metal–organic Framework Materials for Light-Harvesting and Energy Transfer. *Chem. Commun.* **2015**, *51* (17), 3501–3510.

(73) Williams, D. E.; Rietman, J. A.; Maier, J. M.; Tan, R.; Greytak, A. B.; Smith, M. D.; Krause, J. A.; Shustova, N. B. Energy Transfer on Demand: Photoswitch-Directed Behavior of Metal–Porphyrin Frameworks. *J. Am. Chem. Soc.* **2014**, *136* (34), 11886–11889.

(74) Park, J.; Feng, D.; Yuan, S.; Zhou, H.-C. Photochromic Metal-Organic Frameworks: Reversible Control of Singlet Oxygen Generation. *Angew. Chemie Int. Ed.* **2015**, *54* (2), 430–435.

(75) Danowski, W.; van Leeuwen, T.; Abdolahzadeh, S.; Roke,

D.; Browne, W. R.; Wezenberg, S. J.; Feringa, B. L. Unidirectional Rotary Motion in a Metal–organic Framework. *Nat. Nanotechnol.* **2019**, *14* (5), 488–494.

(76) Farha, O. K.; Malliakas, C. D.; Kanatzidis, M. G.; Hupp, J. T. Control over Catenation in Metal- Organic Frameworks via Rational Design of the Organic Building Block. *J. Am. Chem. Soc.* **2010**, *132* (3), 950–952.

(77) Madrahimov, S. T.; Atesin, T. A.; Karagiaridi, O.; Sarjeant, A. A.; Farha, O. K.; Hupp, J. T.; Nguyen, S. T. Metal-Organic Frameworks Containing (Alkynyl)gold Functionalities: A Comparative Evaluation of Solvent-Assisted Linker Exchange, de Novo Synthesis, and Post-Synthesis Modification. *Cryst. Growth Des.* **2014**, *14* (12), 6320–6324.

(78) Karagiaridi, O.; Bury, W.; Mondloch, J. E.; Hupp, J. T.; Farha, O. K. Solvent-Assisted Linker Exchange: An Alternative to the de Novo Synthesis of Unattainable Metal-Organic Frameworks. *Angew. Chem. Int. Ed.* **2014**, *53* (18), 4530–4540.

(79) Karagiaridi, O.; Bury, W.; Tylianakis, E.; Sarjeant, A. A.; Hupp, J. T.; Farha, O. K. Opening Metal−Organic Frameworks Vol. 2: Inserting Longer Pillars into Pillared-Paddlewheel Structures through Solvent-Assisted Linker Exchange. *Chem. Mater.* **2013**, *25*, 3499–3503.

(80) Bury, W.; Fairen-Jimenez, D.; Lalonde, M. B.; Snurr, R. Q.; Farha, O. K.; Hupp, J. T. Control over Catenation in Pillared Paddlewheel Metal-Organic Framework Materials via Solvent-Assisted Linker Exchange. *Chem. Mater.* **2013**, *25* (5), 739–744.

(81) Burnett, B. J.; Barron, P. M.; Hu, C.; Choe, W. Stepwise Synthesis of Metal–Organic Frameworks: Replacement of Structural Organic Linkers. *J. Am. Chem. Soc.* **2011**, *133* (26), 9984–9987.

(82) Vinogradov, S. A.; Wilson, D. F. Phosphorescence Lifetime Analysis with a Quadratic Programming Algorithm for Determining Quencher Distributions in Heterogeneous Systems. *Biophys. J.* **1994**, *67*, 2048–2059.

(83) Montalti, M.; Credi, A.; Prodi, L. P.; Gandolfi, M. T. *Handbook of Photochemistry.*, Third.; CRC/Taylor & Francis: Boca Raton, 2006.

(84) Evans, J. D.; Krause, S.; Feringa, B. L. Cooperative and Synchronized Rotation in Motorized Porous Frameworks: Impact on Local and Global Transport Properties of Confined Fluids. *Faraday Discuss.* **2020**.

Photosensitizer

Molecular Motor

530 nm

Energy Transfer